Direct observation of space charge induced hydrogen ion insertion in nanoscale anatase TiO_2†

Wing K. Chan, Wouter J. H. Borghols and Fokko M. Mulder*

Received (in Cambridge, UK) 18th July 2008, Accepted 2nd October 2008
First published as an Advance Article on the web 30th October 2008
DOI: 10.1039/b812311j

Space charge induced $^2H^+$ densities up to $^2H^+_{0.17}TiO_2$ are observed directly using neutron diffraction on two different nanoscale particle sizes of anatase TiO_2 immersed in sulfuric acid, and consistent with experimental evidence modelling shows that these ions show rapid self diffusion.

Recently it has been shown that solid acid super protonic conductors that can be applied as fuel cell electrolytes[1] can show enhanced conductivities by blending with nanoparticulates like TiO_2 and SiO_2.[2–7] Fuel cell membranes made of hybrid organic–inorganic nanocomposites consisting of Nafion and anatase TiO_2 were recently reported[8] and exhibit good proton conductivities and extended operation temperatures. Not much is known about the charge transport and ionic densities that are present in the nanofilled materials like TiO_2, although there are indications that such materials can play a role in the ion transport itself. For instance it was also shown recently that 18 nm thick TiO_2 layers can transport protons[9] at temperatures as low as 80 °C in a fuel cell configuration. In order to investigate the hydrogen density and transport inside such nano fillers we present here a study on hydrogen inside TiO_2 nanoparticles immersed in sulfuric acid.

An important factor influencing the ionic densities and conductivity of nanostructured ionic conductors in general is the presence of so-called space charge effects.[10,11] The basic mechanism responsible for the creation of space charges is the difference in chemical potential that charged ions have in the different ionic compounds that are in close contact in a nanocomposite. This difference drives charged ions from one phase to the other, breaking charge neutrality at the interface. The ion flow stops as soon as the electric field that builds up counterbalances the difference in chemical potential. The length scale involved in these interface effects is typically of the order of few tens of nm (Debye length). When the crystallite sizes of the different ionic phases becomes of the order of this space charge layer thickness, the entire particle becomes influenced by the space charge induced ionic density changes and one can then speak of true nanoscale size effects.[11] The effect of the space charges on the ionic conductivity is mainly due to the abundant vacancies and the introduction of mobile ions in the space charge regions of the material. For this reason we investigate here by a direct probe, neutron diffraction, the density of hydrogen inserted in nanoscale TiO_2 crystallites when immersed in concentrated sulfuric acid. Sulfuric acid is used because in sulfonated polymer membranes H_2SO_4 is used to activate the proton conductivity.[12] Because of its acidic nature the proton has a high chemical potential in the acid and space charges can be expected to build up. The result for the location of the inserted ions is compared to *ab initio* calculations, and force field molecular dynamics simulations are used to estimate the mobility of the ions. To the best of our knowledge this is the first time that the induced ionic density is observed directly.

TiO_2 nanopowders with average size of 7 nm (obtained from NanoAmor) and 24 nm (Nanoaltair) were dried in a vacuum oven and subsequently immersed in liquid D_2SO_4 (98 wt% solution in D_2O, 99.5+ atom% D). Deuterium is used because proton-containing samples have an unwanted high background in neutron diffraction due to the large incoherent cross-section of ^1H. Neutron diffraction was performed using GEM at ISIS, Rutherford Appleton Laboratories (Oxfordshire, UK). The particle sizes from the neutron diffraction line broadening were consistent with electron microscopy. Liquid D_2SO_4 was used in order to prevent overlapping with spectra of another crystalline phase in this first study that will be used as a benchmark for other studies. The samples were measured at room temperature and the tubes were sealed airtight to prevent exchange of deuterium with protons in humid air. The diffraction data were analyzed with the Rietveld method using the software GSAS.[13] Three dimensional (difference) Fourier maps were generated using the program Fox[14] in order to elucidate the position of inserted density of deuterons within the structure.

Fig. 1 shows the diffraction spectra of the 24 nm TiO_2 samples, with and without D_2SO_4. The differences between the spectra are small, but with the high statistics clearly detectable (Table 1).

In Fig. 2 the resulting Fourier map of the 24 nm sample in D_2SO_4 is shown. Apart from the Ti and O atoms from TiO_2 there are clear high density spots visible due to the presence of inserted D ions. This density is located at [0.00, 0.75, 0.43] (fractional coordinates). The distance between the deuteron and the nearest oxygen atom is 0.92 Å. Such distance is comparable to the distance of 0.95 Å between O and H in an OH^- group. The position as well as the occupancy and temperature factor of this deuteron density was refined. The result was a clearly better agreement between the data and the fitted spectrum (5% lower R factor *vs.* fit without D, wR_p: 0.0044, 24 nm sample). Both TiO_2 particle sizes, 24 nm and 7 nm, were analyzed in this way resulting in occupancies of

Fundamental Aspects of Materials and Energy, Department of Radiation, Radionuclides, and Reactors, Faculty of Applied Sciences, Delft University of Technology, Mekelweg 15, 2629JB Delft, The Netherlands. E-mail: f.m.mulder@tudelft.nl

† CCDC 695519. For crystallographic data in CIF or other electronic format see DOI: 10.1039/b812311j

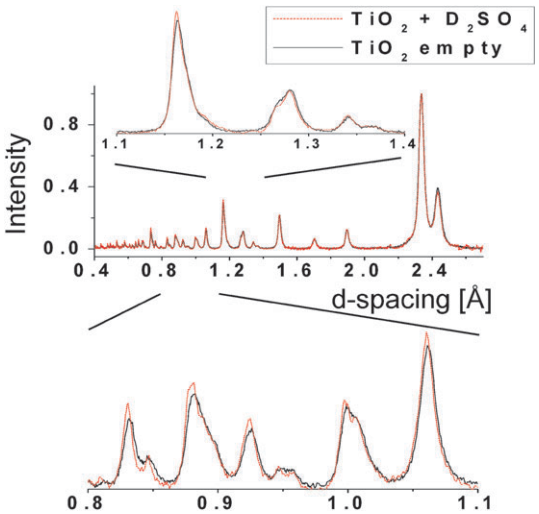

Fig. 1 Diffraction spectra of 24 nm TiO_2 before and after immersion in D_2SO_4, normalised at the largest peak intensity. Subtle changes in peak intensities occur that give direct information on the location and density of deuterium nuclei in the TiO_2 lattice.

Table 1 Refined structure of 24 nm anatase D^+ inserted TiO_2 in D_2SO_4 at 293 K. The space group is I41/amd (space group no. 141) with $a = 3.785$ Å and $c = 9.508$ Å

Atom	X	Y	Z	U_{iso} [Å^2]	Occupancy
Ti	0	3/4	1/8	0.005 ± 0.005	1
O	0	3/4	0.3301	0.007 ± 0.005	1
D	0	3/4	0.43	0.06 ± 0.01	0.045 ± 0.005

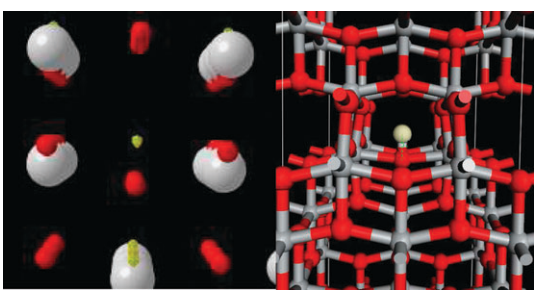

Fig. 2 (Left) Fourier difference map showing the deuteron position (yellow shape) from the diffraction experiments (Ti: gray, oxygen: red). (Right) Calculated H position using VASP. It can be seen that the position resulting from the calculations is the same as the one from the diffraction experiments.

0.045 for the former and 0.085 for the latter. This translates in deuteron intercalation of respectively 0.09 and 0.17 per TiO_2.

We calculated the position of protons in TiO_2 using the density functional approach as implemented in the *ab initio* package VASP.[15] Standard pseudopotentials in the Generalised Gradient Approximation (GGA) for Ti, O, and H were used. The structure of a $2 \times 2 \times 2$ TiO_2 supercell including one proton was minimised in order to determine the minimum energy position of the H. The calculations show a position as in Fig. 2, with a distance of the proton to the oxygen of 0.99 Å. This position is in very good agreement with the results from the diffraction experiments. There are two equivalent sites in the oxygen octahedron with a splitting of 3.95 Å between them. It is essential to use a model in which the H density is not higher than experimentally observed because for high H densities the H atoms will start interacting, which will influence the structure. It is interesting to note that such a split position of the H is similar to that of intercalated Li in $Li_{0.02}TiO_2$ anatase:[16] there too Li chooses one of two positions well above and below the centre of the oxygen octahedron. This split position of the Li ion inside the oxygen octahedron can also be reproduced by VASP in the same $2 \times 2 \times 2$ model with a Li position of (0, 0.75, 0.520) (this result was not yet reported in ref. 16 but it compares well with the experimental Li position of (0, 0.75, 0.5401)). The distance between the Li and its oxygen neighbour is 1.80 Å, *i.e.* much larger than the D–O distance, while the splitting between the two Li positions is reduced to 1.92 Å compared to the D–D splitting of 3.95 Å.

The experimentally observed D position agrees with the theoretically predicted one. This indicates that such modelling can reproduce the relevant factors in the structure. In order to model the diffusion of H through the structure using molecular dynamics simulations the *ab initio* method is too calculationally intensive. For this reason we used the *ab initio* based parameterised force field method COMPASS[17] as implemented in Materials Studio.[18] COMPASS reproduces the minimal energy position of the H atom from the experiment and from VASP. With a time step of 1 fs simulations of the same model were made as above for durations of up to 1200 ps at various temperatures. In Fig. 3 an Arrhenius plot is given of the observed hopping rates. The error bars in the graph are calculated as the square root of the observed discrete number of hops. Two types of hops of the H atoms are observed: a small hop inside the same octahedron along the *c*-axis and a long hop from (the bottom position in) one octahedron to (the top in) a nearest neighbour one. The activation energies resulting from the fits are 1.7×10^3 K and 2.4×10^3 K for the intra- and inter-hopping rates respectively. The temperature dependencies of the simulated hopping rates ($1/\tau_{intra}$, $1/\tau_{inter}$) equal respectively $1.50 \exp[-1.7 \times 10^3/T]$ and $1.37 \exp[-2.4 \times 10^3/T]$ ps^{-1} for the intra- and inter-octahedron hops. The long range H diffusion may be viewed as a two step process of relatively fast intra-octahedron hops and approximately an order of magnitude slower nearest neighbour octahedron hops. The diffusion coefficient D can be estimated from the inter-octahedron hopping time τ and the average distance l

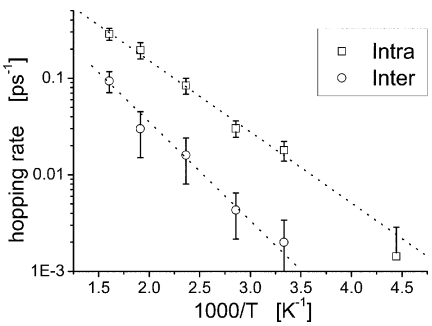

Fig. 3 Arrhenius plot of the predicted hopping rate of a proton in TiO_2 as a function of temperature. The inter-octahedron hopping rate determines the long range diffusive motion since the intra-octahedron hopping model is relatively fast.

between two sites in nearest neighbour octahedrons as follows: $D = l^2/4\tau_{inter}$, which equals 0.91×10^{-7} cm^2 s^{-1} at 300 K. Such value is only a factor of three smaller than Nafion at 300 K as reported in *e.g.*[19,20] at 20% relative humidity,[21] which may indicate that the diffusion of these protons in anatase nanoparticles is in itself high enough for fuel cell applications at 300 K. At increasing temperatures this only improves.

It is interesting to note that in the previous study on Li insertion in anatase TiO_2 mentioned above[16] it was also found both experimentally and by using the force field modelling based on COMPASS that the Li position inside the oxygen octahedron was split in two positions. In that study the hopping of the Li ion between these two intra-octahedron positions predicted by COMPASS was also observed directly using quasielastic neutron scattering.

An important observation that indicates that the TiO_2 has taken up positively charged deuterium ions is that the material has not changed colour. Upon neutral H and Li insertion in TiO_2 the electric and optical properties change significantly.[22–24] Upon neutral H insertion a deep electronic energy level is created at 0.52 eV inside the bandgap of 3.75 eV. This leads to strong absorption in the visible light and a blue coloration of the material. With Li insertion this can directly be observed as the original white powder turns blue. In contrast these nanoparticle powders keep their white refracting appearance indicating that the deep levels at 0.52 eV are still unoccupied, *i.e.* the electrons accompanying the deuterium nucleus are missing. Therefore the observed deuterium ion insertion leads to the build up of a space charge.

In principle such a space charge layer extends only a finite length into the TiO_2. The Rietveld refinement assumes a constant average D density, and from the two particle sizes measured and the observed average D insertion density a rough estimate can be made of the typical length scale of the D insertion: a 24/7 times larger particle has on average 0.17/0.09 times less D inserted. Using an exponential decay from the surface these numbers are consistent with a typical length scale for insertion of $\sim$11 nm with a typical maximum D insertion amplitude of $\sim$0.25 at the surface.

Enhancing ionic conduction due to space charge effects can be beneficial for *e.g.* proton conductors in fuel cell applications. Especially the application as electrolyte membrane in fuel cells operating at intermediate temperatures (120–250 °C), where conventional membranes based on humidified hydrophilic polymers are unable to operate,[25] can be considered very promising.[11] Intermediate temperatures are favourable for three reasons. First, the higher temperatures facilitate the utilisation of the waste heat, enhancing the overall energy efficiency. Second, the higher temperatures reduce the sensitivity of the catalysts used to CO poisoning. Third, the higher temperature makes cooling against the ambient environment less technologically demanding.

Assistance from Dr W. A. Kockelmann at the ISIS facility is gratefully acknowledged. Financial support for ISIS beam time was obtained from the Netherlands Organization for Scientific Research (NWO). This article is the result of joint research in the Delft Research Centre for Sustainable Energy and the 3TU. Centre for Sustainable Energy Technologies.

Notes and references

1 S. M. Haile, D. A. Boysen, C. R. I. Chisholm and R. B. Merle, *Nature*, 2001, **410**, 910.
2 V. G. Ponomareva, G. V. Lavrova and L. G. Simonova, *Solid State Ionics*, 1999, **118**, 317.
3 V. G. Ponomareva, N. F. Uvarov, G. V. Lavrova and E. F. Hairetdinov, *Solid State Ionics*, 1996, **90**, 161.
4 V. G. Ponomareva and G. V. Lavrova, *Solid State Ionics*, 1998, **106**, 137.
5 V. G. Ponomareva, G. V. Lavrova and L. G. Simonova, *Solid State Ionics*, 1999, **119**, 295.
6 J. Otomo, N. Minagawa, C. Wen, K. Eguchi and H. Takahashi, *Solid State Ionics*, 2003, **156**, 357.
7 S. Wang, J. Otomo, M. Ogura, C. Wen, H. Nagamoto and H. Takahashi, *Solid State Ionics*, 2005, **176**, 755.
8 A. Saccà, *et al.*, *J. Power Sources*, 2005, **152**, 16–21.
9 H. Ekström, B. Wickman, M. Gustavsson, P. Hanarp, L. Eurenius, E. Olsson and G. Lindbergh, *Electrochim. Acta*, 2007, **52**, 4239–4245.
10 N. Sata, K. Eberman and J. Maier, *Nature*, 2000, **408**, 946.
11 J. Maier, *Nature Materials*, 2005, **4**, 805.
12 M. L. Di Vona, *et al.*, *J. Membrane Science*, 2007, **296**, 156–161.
13 A. C. Larson and R. B. Dreele, ''General Structure Analysis System (GSAS)'', LAUR 86-748, Los Alamos National Laboratory, 1994.
14 V. Favre-Nicolin and R. Cerny, *J. Appl. Cryst.*, 2002, **35**, 734–743. Available from http://objcryst.sourceforge.net.
15 VASP, ''Vienna *Ab initio* Simulation Package'', G. Kresse and J. Furthmüller, *Phys. Rev. B*, 1996, **54**, 11169; G. Kresse and J. Furthmüller, *Comp. Mat. Sci.*, 1996, **6**, 1; G. Kresse and D. Joubert, *Phys. Rev. B*, 1999, **59**, 1758.
16 M. Wagemaker, G. J. Kearley, A. A. van Well, H. Mutka and F. M. Mulder, *J. Am. Chem. Soc.*, 2003, **125**, 840–848.
17 H. Sun, *J. Phys. Chem.*, 1998, **102**, 7338.
18 Materials studio is a software environment developed by Accelrys.
19 K. D. Kreuer, S. J. Paddison, E. Spohr and M. Schuster, *Chem. Rev.*, 2004, **104**(10), 4637–4678.
20 A. Venkatnathan, R. Devanathan and M. Dupuis, *J. Phys. Chem. B*, 2007, **111**, 7234–7244.
21 P. J. James, J. A. Elliott, T. J. H. H. Wills, J. M. Newton, A. M. S. Elliott, S. Hanna and M. J. Miles, *J. Mater. Sci.*, 2000, **35**, 5111–5119.
22 C. Bechinger, S. Ferrere, A. Zaban, J. Sprague and B. A. Gregg, *Nature*, 1993, **383**, 608–610.
23 M. Wagemaker, A. A. van Well, G. J. Kearley and F. M. Mulder, *Solid State Ionics*, 2004, **175**, 191.
24 M. Wagemaker, A. P. M. Kentgens and F. M. Mulder, *Nature*, 2002, **418**, 397–399.
25 F. De Bruijn, *Green Chem.*, 2005, **7**, 132.

